LETTERS
PUBLISHED ONLINE: 9 NOVEMBER 2015 | DOI: 10.1038/NMAT4465
nature materials

# Activating and optimizing $MoS_2$ basal planes for hydrogen evolution through the formation of strained sulphur vacancies

Hong Li[1†], Charlie Tsai[2,3†], Ai Leen Koh[4], Lili Cai[1], Alex W. Contryman[5,6], Alex H. Fragapane[5,6], Jiheng Zhao[1], Hyun Soo Han[1], Hari C. Manoharan[5,7], Frank Abild-Pedersen[3], Jens K. Nørskov[2,3*] and Xiaolin Zheng[1*]

NATURE MATERIALS | VOL 15 | JANUARY 2016 | www.nature.com/naturematerials

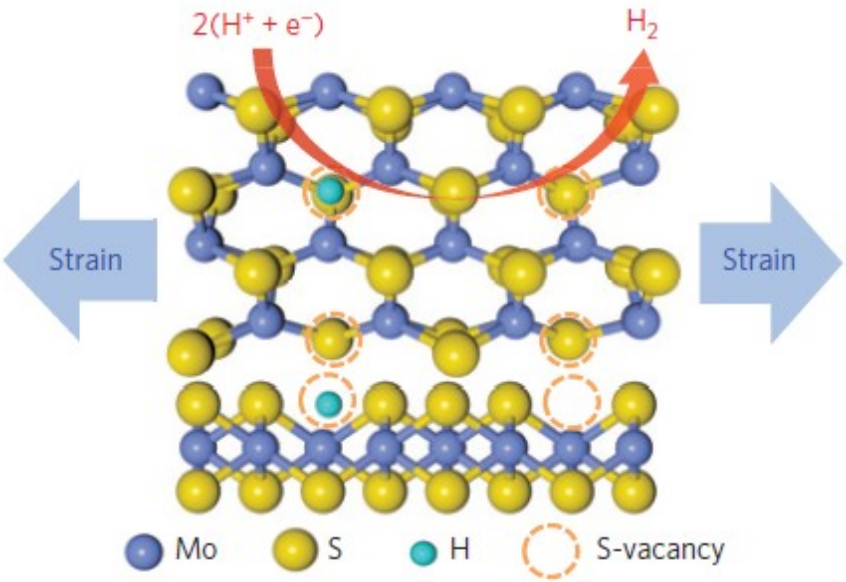


By
Biswajit
23-07-2016

# Introduction

- Owing to its relatively low cost, earth abundance, high catalytic activity and good stability, $MoS_2$ is a promising alternative to platinum (Pt) for catalysing electrochemical hydrogen ($H_2$) production from water.

- Active edge sites of $MoS_2$ are responsible for the HER activity over the inactive basal plane.

- One strategy focuses on maximally exposing edge sites using nanostructured $MoS_2$, such as nanoparticles, vertical nanoflakes, nanowires, defect-rich films or mesoporous films.

- Another strategy strives to enhance the intrinsic activity of the edge sites by atomic-scale modifications such as chemical doping.

# In this paper

- Here they reported the first successful activation and optimization of the basal plane of monolayer 2H-$MoS_2$ by creating and straining S-vacancies.

- Density functional theory (DFT) calculations indicate that S-vacancies introduce gap states that allow favourable hydrogen adsorption and increasing the number of S-vacancy sites strengthens hydrogen adsorption.

# Result and discussion

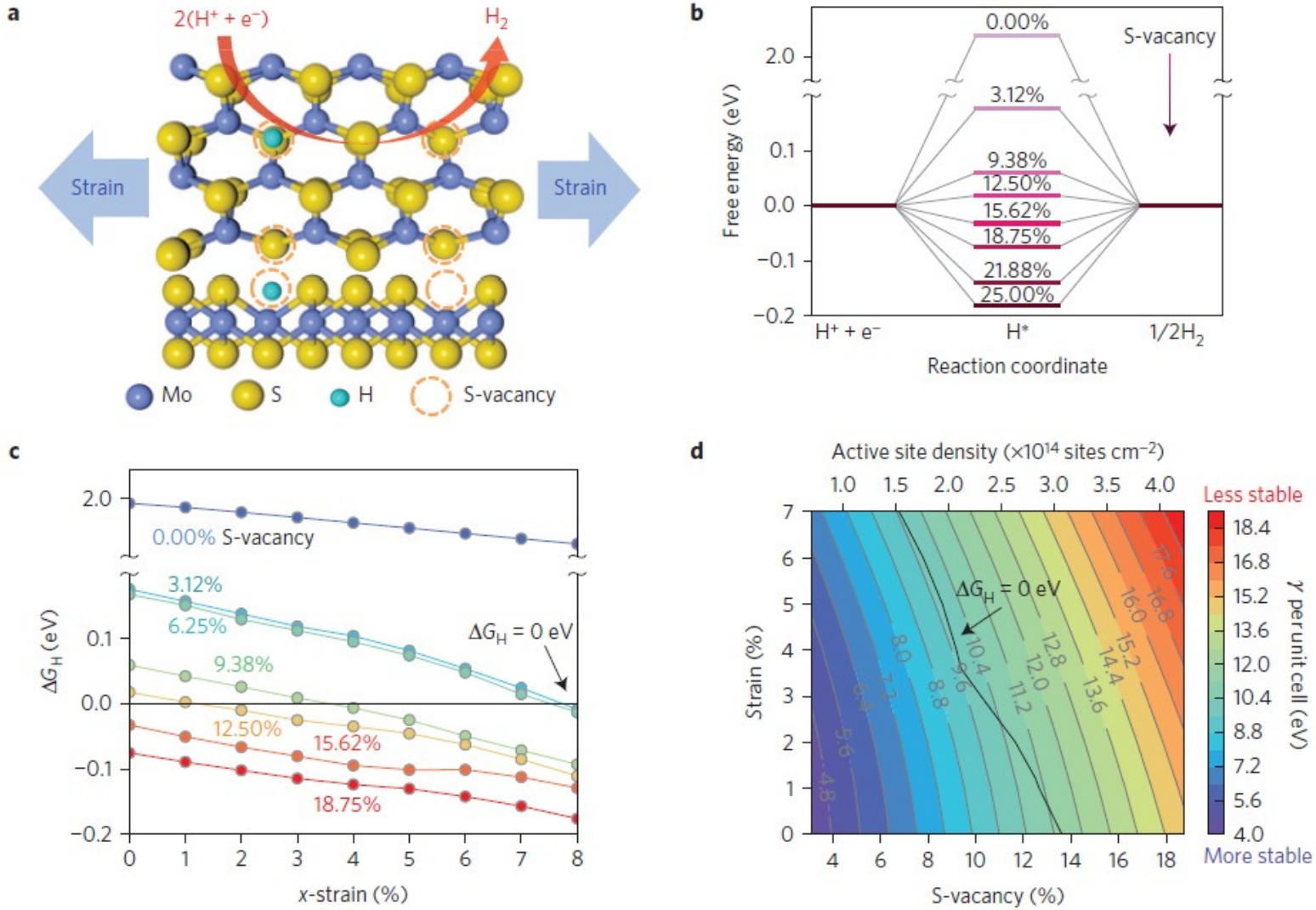


**Figure 1 | Theoretical calculations for the effects of S-vacancies and strain on the HER activity of $MoS_2$. a**, Schematic of the top (upper panel) and side (lower panel) views of $MoS_2$ with strained S-vacancies on the basal plane, where S-vacancies serve as the active sites for hydrogen evolution and applied strain further tunes the HER activity. **b**, Free energy versus the reaction coordinate of HER for the S-vacancy range of 0–25%. **c**, $\Delta G_H$ versus %*x*-strain for various %S-vacancy, ranging from 0.0% (pristine) to 18.75%. **d**, Coloured contour plot of surface energy per unit cell $\gamma$ (with respect to the bulk $MoS_2$) as a function of S-vacancy and uniaxial strain. Colour bar represents the value of $\gamma$. The black lines in **c** and **d** indicate combinations of S-vacancy and strain that yield $\Delta G_H = 0$ eV, the optimal thermodynamic requirement for HER activity.

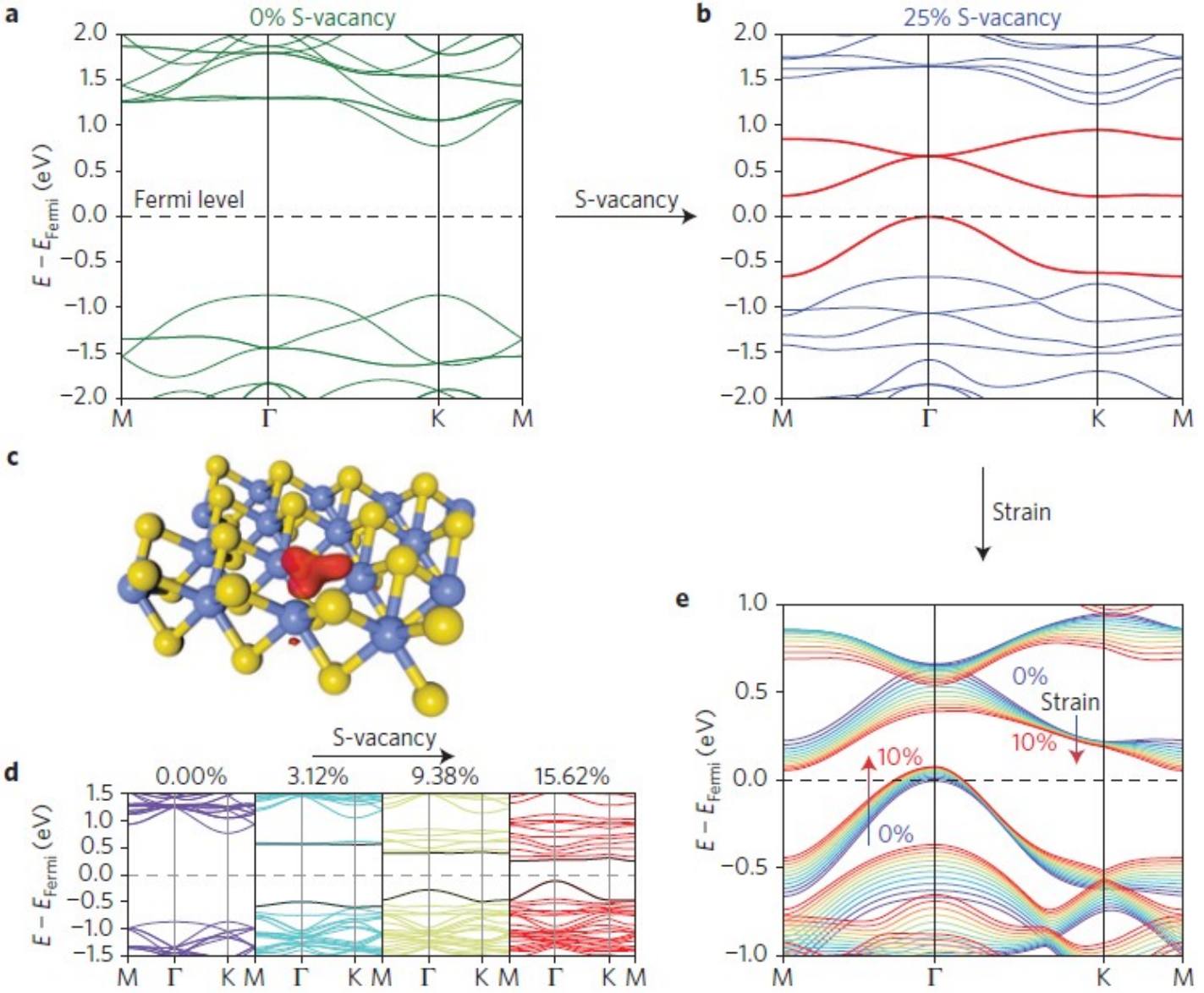


**Figure 2 | Effects of S-vacancy and strain on the electronic structure of $MoS_2$. a**,**b**, Band structure of monolayer 2H-$MoS_2$ with 0% (**a**) and 25% S-vacancies (**b**) (calculated using a reduced $2 \times 2$ unit cell for clarity). S-vacancies introduce new bands (red curves) in the gap, near the Fermi level. **c**, Kohn–Sham orbitals (red) corresponding to the new bands just below the Fermi level are localized around the S-vacancy. **d**, Tuning of the band structure due to increasing S-vacancy concentrations (calculated using the full $4 \times 4$ unit cell). The bands nearest to the Fermi level are highlighted in black and the extra bands are due to the larger unit cell size needed to reflect the smaller S-vacancy concentrations. **e**, Fine-tuning of the band structure for 25% S-vacancy under applied strain. With increasing strain, the bands approach the Fermi level, resulting in the narrowing gap.

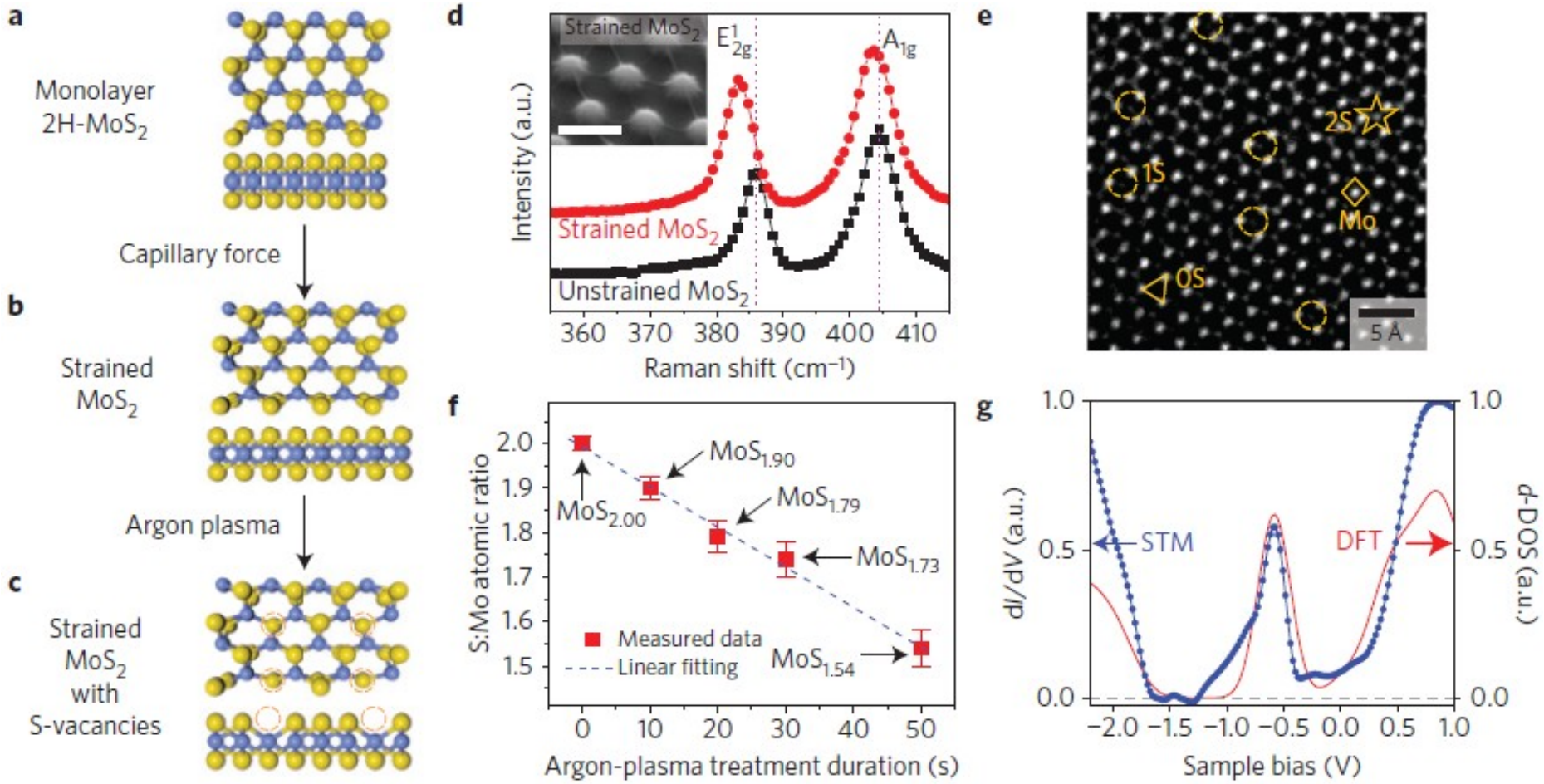


**Figure 3 | Experimental creation and quantification of S-vacancies and elastic tensile strain in monolayer 2H-$MoS_2$. a–c**, Schematic of the top (top panel) and side (lower panel) views of pristine monolayer 2H-$MoS_2$ (**a**), strained $MoS_2$ (**b**) and strained $MoS_2$ with S-vacancies (**c**). Arrows illustrate the key experimental processes involved. **d**, Representative Raman spectra for the unstrained and strained $MoS_2$. Dotted lines indicate the positions of the $E^1_{2g}$ and $A_{1g}$ peaks for unstrained $MoS_2$. Inset: tilted SEM image of strained $MoS_2$. Scale bar is 500 nm. **e**, ACTEM image of a $4 \times 4\,nm^2$ $MoS_2$ monolayer with about 43 S-vacancies (~11.3% S-vacancy). The biggest and brightest dots (rhombus) are Mo atoms. Small bright dots (star), small dim dots (circle), and dark spots (triangle) correspond to a pair of S atoms (2S, one S atom above and the other below the Mo plane), a single S atom (1S, only one S atom below the Mo plane) and zero S atoms (0S, both top and bottom S atoms removed), respectively. **f**, The S:Mo atomic ratio decreases with increasing duration of Ar-plasma treatment, as obtained from XPS measurements. **g**, STM/STS measured d*I*/d*V* (left *y*-axis) and DFT calculated projected *d*-orbital density of states on the Mo atom of the S-vacancy (right *y*-axis) versus sample bias for the S-vacancy sites (under 12.5% S-vacancy). The STS spectrum is an average over eight individual spectra. The STM results are in close agreement with DFT results calculated using the GLLB-sc functional corrected for a Fermi level shift of −1.2 eV due to doping.

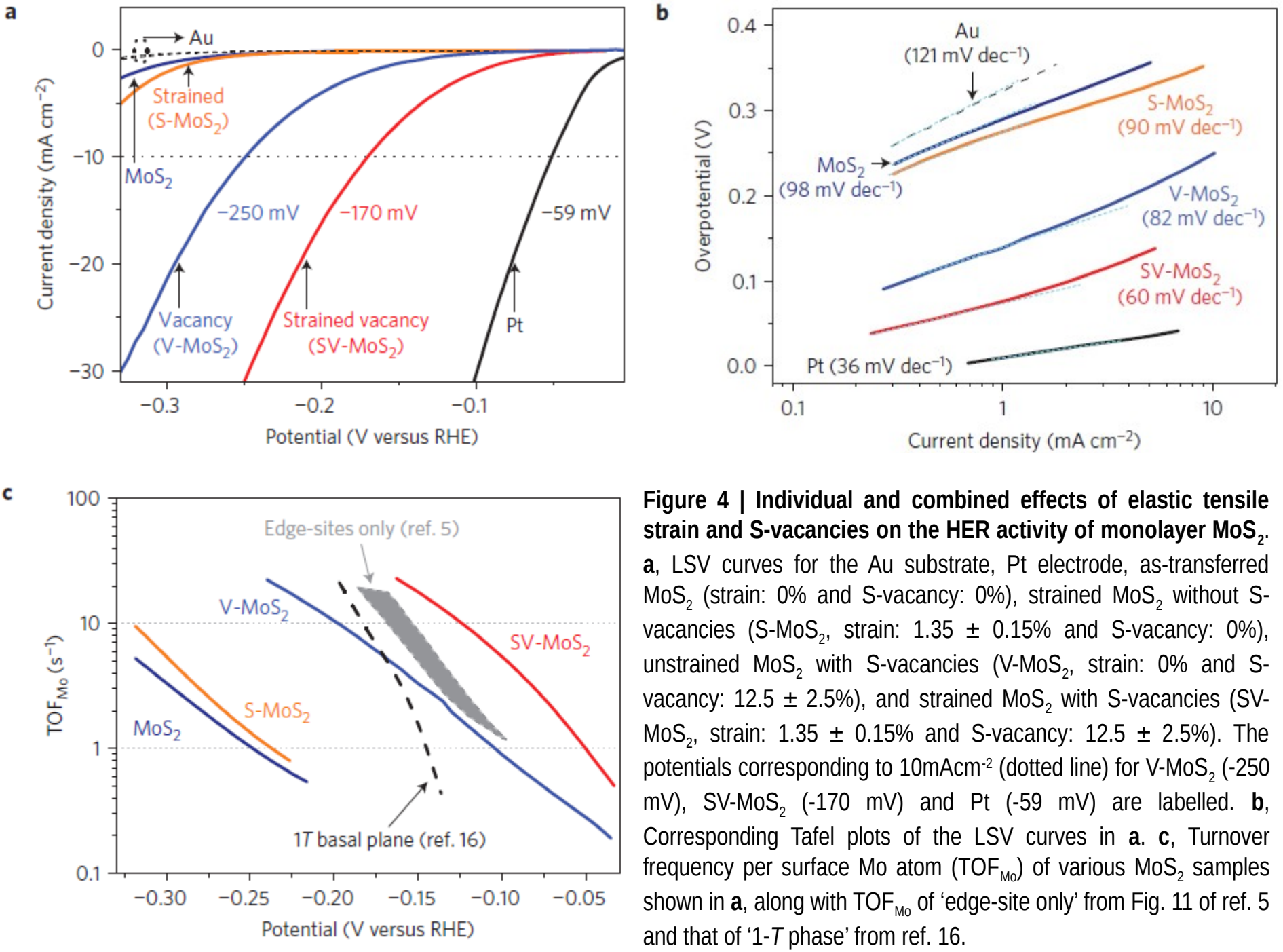


**Figure 4 | Individual and combined effects of elastic tensile strain and S-vacancies on the HER activity of monolayer $MoS_2$.** **a**, LSV curves for the Au substrate, Pt electrode, as-transferred $MoS_2$ (strain: 0% and S-vacancy: 0%), strained $MoS_2$ without S-vacancies (S-$MoS_2$, strain: 1.35 ± 0.15% and S-vacancy: 0%), unstrained $MoS_2$ with S-vacancies (V-$MoS_2$, strain: 0% and S-vacancy: 12.5 ± 2.5%), and strained $MoS_2$ with S-vacancies (SV-$MoS_2$, strain: 1.35 ± 0.15% and S-vacancy: 12.5 ± 2.5%). The potentials corresponding to 10mAcm$^{-2}$ (dotted line) for V-$MoS_2$ (-250 mV), SV-$MoS_2$ (-170 mV) and Pt (-59 mV) are labelled. **b**, Corresponding Tafel plots of the LSV curves in **a**. **c**, Turnover frequency per surface Mo atom ($TOF_{Mo}$) of various $MoS_2$ samples shown in **a**, along with $TOF_{Mo}$ of 'edge-site only' from Fig. 11 of ref. 5 and that of '1-*T* phase' from ref. 16.

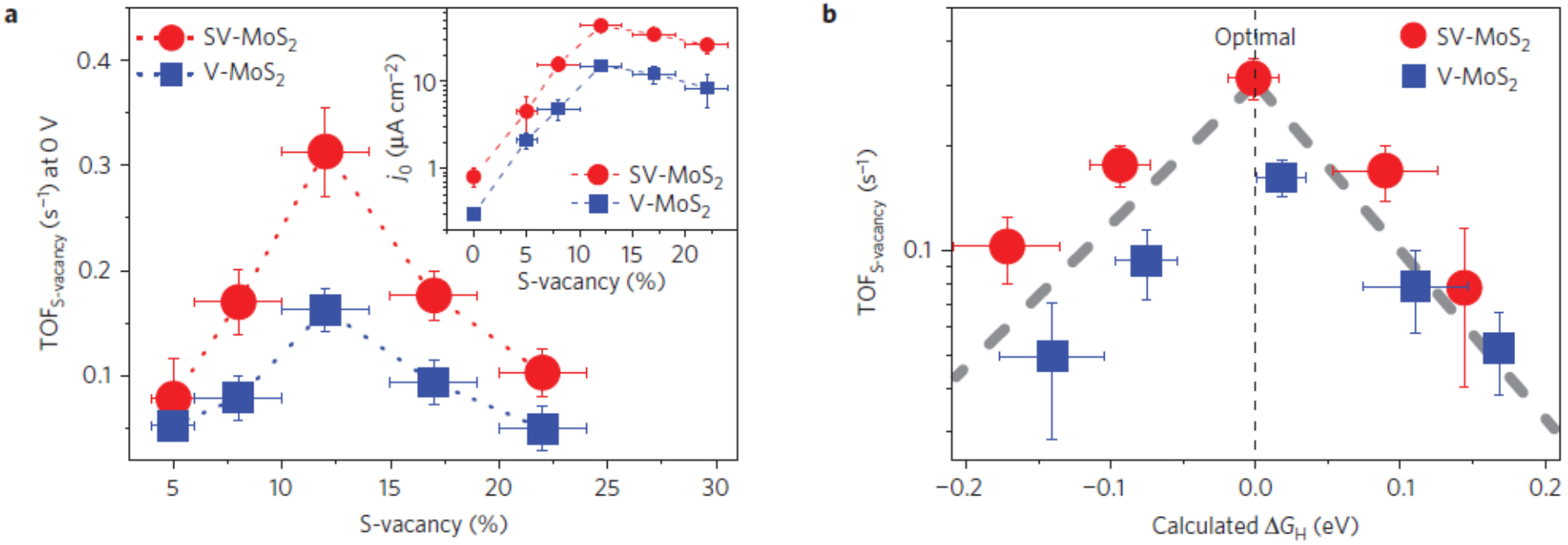


**Figure 5 | Correlation of the intrinsic HER activity of S-vacancy sites between experiments and calculations. a**, Turnover frequency per S-vacancy ($TOF_{S\text{-}vacancy}$) at 0V versus RHE as a function of %S-vacancy for V-$MoS_2$ and SV-$MoS_2$. The strained samples have 1.35 ± 0.15% strain. Inset: exchange current density $j_0$ as a function of %S-vacancy for V-$MoS_2$ and SV-$MoS_2$. **b**, Experimental $TOF_{S\text{-}vacancy}$ versus their corresponding calculated $\Delta G_H$ for V-$MoS_2$ and SV-$MoS_2$. They follow a volcano relation (dashed lines) with the peak at $\Delta G_H$= 0 eV. The $\Delta G_H$ values were calculated at 21.88%, 18.75%, 12.50%, 8.00% and 6.25% S-vacancy (left to right on the plot) and with either 0% or 1.35% applied strain. The error bars in the $TOF_{S\text{-}vacancy}$ represent variations in the experimental samples (Supplementary Fig. 11) and the error bars in

# In summary

- They have theoretically predicted and then experimentally verified that strained S-vacancies in the basal plane of 2H-phase monolayer $MoS_2$ act as a new highly active and tunable catalytic site for HER.

- This is the first account of using S-vacancies in the basal plane to introduce gap states, which can be varied using the S-vacancy concentration and elastic strain.

# Future direction

- If we spray $AgNO_3$ solution, it will create s-vacancies by reacting with $MoS_2$. Then we can use this materials for water splitting.